KINETICS OF CONFORMATIONAL CHANGES IN tRNA^Phe (YEAST) AS STUDIED BY THE FLUORESCENCE OF THE Y-BASE AND OF FORMYCIN SUBSTITUTED FOR THE 3'-TERMINAL ADENINE

Stephen M. COUTTS*, Detlev RIESNER, Roland RÖMER,
Carl R. RABL** and Guenter MAASS

*Institut für Klinische Biochemie und Physiologische Chemie, Medizinische Hochschule Hannover,
D-3 Hannover, West Germany,
and Gesellschaft für Molekularbiologische Forschung mbH, Stoeckheim/Braunschweig, West Germany*

The kinetics of the melting transitions of tRNA^Phe (yeast) were followed by the fluorescence of the Y-base and of formycin substituted for the 3'-terminal adenine. As judged from differential UV absorbance melting curves the formycin label had virtually no influence on the conformation of the tRNA. A temperature jump apparatus was modified to allow the simultaneous observation of transmission and fluorescence intensities by two independent optical channels. The design of a temperature jump cell with an all quartz center piece is given. The cell is resistant to temperatures up to 90°C; it provides high optical sensitivity, low stray light intensity and the possibility of measuring fluorescence polarization. The T-jump experiments allowed to discriminate between fast unspecific fluorescence quenching ($\tau < 5\,\mu sec$) and slow co-operative conformational changes. In the central part of the temperature range of UV-melting (midpoint temperature 30°C in 0.01 M Na^+ and 39°C in 0.03 M Na^+, pH 6.8) two resolvable relaxation processes were observed. The corresponding relaxation times were 20 msec and 800 msec at 30°C in 0.01 M Na^+, and 4 msec and 120 msec at 39°C in 0.03 M Na^+. The Y-base fluorescence shows both of the relaxation effects, which almost cancel in equilibrium fluorescence melting, because their amplitudes have opposite signs. From this finding the existence of some residual tertiary structure is inferred which persists after the unfolding of the main part of tertiary structure during early melting (midpoint temperature 24°C in 0.03 M Na^+). In the fluorescence signal of the formycin also the two relaxation effects appear. Both of them are connected with a decrease of the fluorescence intensity. From the results a coupled opening of the anticodon and acceptor branches is concluded.

Enzymes: phenylalanyl-tRNA synthetase, PRS (EC 6.1.1.—20); ATP (CTP) tRNA nucleotidyl transferase, NT (EC 2.7.7.—20); alkaline phosphatase (EC 3.1.3.1).

Abbreviations: tRNA^Phe$C_{74}C_{75}A_{76}$ is native phenylalanine specific tRNA from yeast; tRNA^Phe$C_{74}C_{75}$ is native phenylalanine tRNA with the 3'-terminal adenosine-5'-phosphate removed; tRNA^Phe$C_{74}C_{75}F_{76}$ is phenylalanine tRNA with formycin substituted for the 3'-terminal adenosine in position 76; FTP is formycin-5'-triphosphate, where the structure of formycin is 7-amino-3 (β-D-ribofuranosyl) pyrazolo (4.3-d) pyrimidine; A_λ unit is that quantity of material which, when dissolved in 1.0 ml of solvent has an absorbance of 1.0 at λ nm for a 1.0 cm pathlength at 20°C; EDTA is ethylenediamine tetraacetic acid.

1. Introduction

General aspects of conformational transitions in

* Present address: Dept. of Biochemical Sciences, Princeton University, Princeton N.J. 08540, U.S.A.
** Present address: Max-Planck Institut für Biophysikalische Chemie, D-34 Göttingen, Germany.

tRNA's and their biological relevance have been extensively reviewed [1,2]. In phenylalanine specific tRNA from yeast, five individual conformational transitions have been resolved and their thermodynamic and kinetic behaviour partially characterized [3]. Transition 1 or "early melting", as defined in fig. 8, represents the unfolding of the tertiary structure [4,5]. Transition 4 and 5 can be assigned to the dis-

sociation of the rT- and hU-stems, respectively (figs. 1 and 8). Thus far, however, there has been only indirect proof that the melting of the acceptor- and anticodon stems occurs in the temperature range of transitions 2 and 3 (i.e., the temperature range of transition 2 and 2D in earlier notation), which have nearly identical midpoint temperatures. Therefore, it was desirable to apply methods which make it possible to follow each transition separately. Considerable progress has been recently achieved in the assignment of NMR signals to defined base-pairs [6]; another approach is the use of fluorescence labels [7–12]. In this paper we have utilized the fluorescence of the Y-base to follow the denaturation of the anticodon branch of tRNA^Phe (yeast). Additionally the 3'-terminal adenosine has been replaced by its fluorescent analog formycin to enable a direct observation of the unfolding of the acceptor branch.

We have found that fast kinetic techniques are a valuable tool in analysing the signals of the fluorescent labels, since the techniques allow a discrimination of slow co-operative conformational changes from fast and unspecific quenching of fluorescence. In our kinetic measurements we have employed a fluorescence

temperature jump apparatus which has been modified to allow the simultaneous observation of two different fluorescence labels and the absorption signal.

2. Materials and methods

2.1. Chemicals

Tritiated ATP and phenylalanine were purchased from the Radiochemical Center, Amersham, England, while unlabelled ATP and CTP were products of Boehringer, Mannheim, Germany. Formycin-5'-triphosphate was a kind gift of Drs. Jovin, Max Planck Institute of Biophysical Chemistry, Goettingen, Germany, and Ward, Rockefeller University, New York, NY, USA. The crude barium salt of FTP was purified over DEAE cellulose, which was developed with a gradient of triethylammonium bicarbonate (0.01 – 0.3 M), pH 7.5. DEAE cellulose (DE 52) was from H. Reeve Angel & Co., London, England, and Sephadex was purchased from Pharmacia, Frankfurt, Germany. All other chemicals were of the highest grade commercially available, and were purchased from Merck, Darmstadt, Germany.

2.2. Transfer RNA

Phenylalanine specific and unfractionated tRNA from yeast were obtained from Boehringer, Mannheim. An extinction coefficient of 5.7×10^5 cm^{-1} M^{-1} was used to calculate the concentration of tRNA^Phe in 0.1 M Na$^+$-solutions.

2.3. Enzymes

Alkaline phosphatase (E.coli), code BAPF, was obtained from Worthington Biochemical Corporation, Freehold, NJ, USA, and was used without further purification. Phenylalanyl-tRNA synthetase from yeast was donated by Dr. Krauss, from this laboratory, and had a specific activity of 1600 units/mg (1 unit corresponds to the charging of 1 nmole of phenylalanine to tRNA^Phe per minute at 37°C). ATP (CTP) nucleotidyl transferase was isolated from yeast using a procedure similar to that of Sternbach et al. [13]. Active fractions were stored at −30°C in 50% glycerol, and had a specific activity of ca. 700 units/mg, where a unit
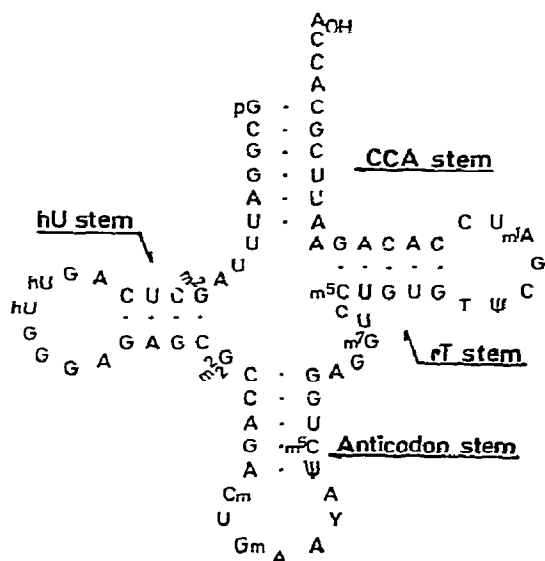

Fig. 1. Clover leaf model of yeast tRNA^Phe according to Raj Bhandary et al. [7].

is defined as the incorporation of 1 nmole of AMP into unfractionated tRNA per minute at 37°C.

2.4. Enzyme assays

The solution used to assay nucleotidyl transferase contained in 100 μl: 40 mM glycine·NaOH, pH 9.0, 8 mM MgSO$_4$, 0.4 mM CTP, 0.42 mM ^{3}HATP (20 mCi/mmole) and 0.1 mg of unfractionated tRNA. The amount of enzyme added was generally from 2 to 6 μg. Samples of 15 μl were withdrawn every 2 minutes, pipetted onto Whatman 3 MM filter paper, quenched in 5% trichloroacetic acid and washed according to Mans and Novelli [14]. The aminoacylation of tRNA^{Phe} and its derivatives was checked by incubating the tRNA in 100 μl of: 50 mM Tris·HCl, pH 7.4, 10 mM ATP, 15 mM MgSO$_4$, 0.1 mM dithiothreitol, 0.1 mM ^{3}HPhe (50 mCi/mmole) and 6 μg of phenylalanyl tRNA synthetase. Reactions were run at 37°C and aliquots were withdrawn after 5, 10 and 15 minutes and treated according to Mans and Novelli.

2.5. Synthesis of tRNA^{Phe}C$_{74}$C$_{75}$F$_{76}$

2.5.1. tRNA^{Phe}C$_{74}$C$_{75}$A$_{76}$

Five mg of tRNA^{Phe} were extracted with phenol, and the aqueous phase chromatographed over G-25 Sephadex, which was eluted with quartz distilled water. The peak fractions were evaporated to dryness,

and the residue dissolved in 5 ml of a solution which contained 50 mM glycine-NaOH, pH 9.0, 10 mM MgSO$_4$, 2 mM ATP, 2 mM CTP and 160 μg of nucleotidyl transferase. This was done to insure the intact 3' sequence of the complete tRNA sample. After 15 minutes at 37°C the solution was extracted with phenol and ether and the tRNA precipitated with alcohol and potassium acetate from the aqueous phase. Residual ATP was stripped from the tRNA by binding the tRNA to a 1 X 7 cm column of DEAE cellulose and washing with 0.3 M NaCl in 0.02 M sodium acetate buffer, pH 5.1. The tRNA was recovered by eluting the column with 1.0 M NaCl in the acetate buffer. The active peak was desalted over G-25 Sephadex. Assays with phenylalanyl tRNA synthetase and nucleotidyl transferase showed that tRNA^{Phe}C$_{74}$C$_{75}$A$_{76}$ could be charged with 1 molecule of phenylalanine, and incorporated about 0.15 molecule of AMP per molecule of tRNA (table 1).

2.5.2. tRNA^{Phe}C$_{74}$C$_{75}$

107 A_{260} units (0.19 μmole) of tRNA^{Phe}C$_{74}$C$_{75}$A$_{76}$ were oxidized with performic acid and the terminal residue removed with aniline as described by Fraenkel–Conrat and Steinschneider [15]. The aniline used in these experiments was distilled over zinc dust, in vacuo, with a nitrogen bleed, shortly before use. A 1.5 hour incubation with alkaline phosphatase (125 μg) in 1.0 ml of 0.02 M Tris·HCL, 1 mM MgSO$_4$, pH 7.8 at 37°C was carried out to cleave the terminal

Table 1
Control experiments to check the completeness of the Whitfield degradation and the incorporation of formycin monophosphate into position 76 of tRNA^{Phe} (yeast)

Sample	Incubation time (min)	Phe/tRNA incorporated by phenylalanyl tRNA synthetase (PRS)	AMP/tRNA incorporated by nucleotidyl transferase (NT)
tRNA^{Phe}C$_{74}$C$_{75}$A$_{76}$	5	1.12	0.13
	10	1.22	0.14
	15	1.23	0.17
tRNA^{Phe}C$_{74}$C$_{75}$	5	0.00 (0.55)[a]	0.98
	10	0.01 (0.96)	1.07
	20	0.03 (0.90)	1.02
tRNA^{Phe}C$_{74}$C$_{75}$F$_{76}$	7	0.56 [b]	0.13
	14	1.03	0.14
	21	0.96	0.18

[a] Values in parentheses refer to assays carried out in the combined presence of 6 μg each of PRS and NT at pH 8.0.

[b] Aminoacylation assays run on tRNA^{Phe}C$_{74}$C$_{75}$F$_{76}$ employed a fivefold higher amount of PRS (30 μg) than was used on the native tRNA^{Phe}.

3' phosphate residue, and was followed by extraction with phenol and chromatography of the aqueous phase over G-25 Sephadex. The yield of tRNA^{Phe}C$_{74}$C$_{75}$ was 93 A_{260} units (87%). Assays carried out on this product with nucleotidyl transferase and phenylalanyl tRNA synthetase demonstrated that 1 AMP and no phenylalanine could be enzymatically incorporated into the 3' terminus. When tRNA^{Phe}C$_{74}$C$_{75}$ was incubated simultaneously with nucleotidyl transferase (NT) and phenylalanyl tRNA synthetase at pH 8, virtually all of the tRNA could be charged with phenylalanine (table 1).

2.5.3. tRNA^{Phe}C$_{74}$C$_{75}$F$_{76}$

60 A_{260} units (140 nmoles) of tRNA^{Phe}C$_{74}$C$_{75}$ and 26 A_{295} units of FTP (2.6 μmoles) were dissolved in 0.90 ml of 1.0 M glycine·NaOH, pH 9.0, containing 10 mM MgSO$_4$. NT (300 μg) was added and the solution was incubated at 35°C for 3 hours, after which it was extracted twice with 0 5 ml of phenol. Non-covalently bound FTP was separated from the tRNA by chromatography over a 1 × 2 column of DEAE Sephadex A-25. The aqueous layer from the phenol extraction was loaded onto the column, which was equilibrated with 0.02 M sodium acetate buffer, pH 5.1. Phenol remaining in the aqueous phase appeared in the breakthrough and water wash. FTP was eluted by washing with 0.3 M sodium chloride in 0.02 M sodium acetate, pH 5.1, and tRNA^{Phe}C$_{74}$C$_{75}$F$_{76}$ was obtained by elution with 1.0 M NaCl. The tRNA peak was treated with 0.03 mmole of EDTA and desalted over a 1 × 60 cm Sephadex G-25 fine column which was developed with quartz distilled water. The yield for this step was 48 A_{260} units (80%). Control experiments with nucleotidyl transferase and phenylalanyl tRNA synthetase demonstrated that the 3'-terminal sequence was intact and could accept phenylalanine.

Particular attention had to be paid to the amount of nucleotidyl transferase used in the synthesis, since high ratios of nucleotidyl transferase to tRNA have been shown to catalyse anomalously high levels of AMP incorporation [16]. Thus, the small amounts of AMP incorporated into tRNA^{Phe}CCA and tRNA^{Phe}CCF probably reflect anomalous incorporation on complete termini.

2.6. Sample preparation

tRNA^{Phe} (yeast) was phenolized and chromato-

graphed on Sephadex G-25 fine at pH 7–8 in the following systems: twice in 0.1 M NaCl, 0.01 M NaEDTA; once in 0.02 M NaCl, 0.2 mM NaEDTA and finally in triply distilled water. This treatment effectively removed Mg^{++} and other divalent ions. As judged by the absence of any effect of EDTA on the melting profiles, the stock solution contained less than one Mg^{++}-ion per tRNA molecule [17]. After diluting the concentrated Mg^{++} free tRNA solution before each experiment the samples were heated to 70°C for 5 min in order to break down aggregates. The measurements were carried out under two ionic conditions: Medium A: 0.01 M Na$^+$-cacodylate; 0.02 M NaCl and 0.001 M NaEDTA at pH 6.8; Medium B: 0.01 M Na$^+$-cacodylate, 0.001 M NaEDTA at pH 6.8. tRNA concentration was between 2 and 6 μM.

2.7. Equilibrium measurements

Differential absorbance melting curves were measured in a Zeiss PMQ II spectrophotometer equipped with two separately thermostated cuvette holders [18]. The temperature dependence of the absorbance of the buffer was substracted from the absorbance changes of the tRNA solutions. $\Delta A(260)/(2°C)$ values were normalized to a total absorbance of 1 (20°C). Peak 1 was separated from the overlapping main melting effect according to

$$\Delta A_1(260) = \Delta A(260)\frac{3.5[1.6 - \Delta A(260)/\Delta A(280)]}{1.9\,\Delta A(260)/\Delta A(280)},$$

(cf. eq. (2) of [18] where $\Delta A_1(260)/\Delta A_1(280) = 3.5$ and $\Delta A_2(260)/\Delta A_2(280) = 1.6$).

Fluorescence spectra were recorded with a Schoeffel RRS 1000 fluorimeter. Fluorescence melting curves were obtained in a Zeiss ZFM4C fluorimeter equipped with two separately thermostated cellholders similar to the setup in the absorbance melting apparatus. The fluorescence intensity (F) was determined relative to the same solution kept at 20 ± 0.2°C. The melting curve was plotted in the differential form $(1/F) \times (\Delta F/\Delta T)$ for easy comparison with the T-jump amplitudes.

2.8. Temperature-jump measurements

Fast kinetic measurements were carried out using a fluorescence temperature-jump apparatus [19,20]. This instrument was modified in order to follow simultaneously the transmission intensity and the
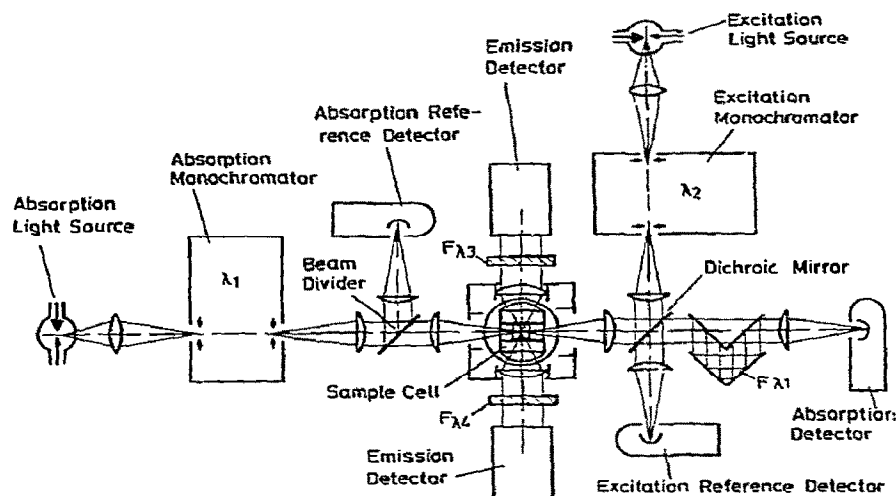
Fig. 2. Dual-wavelength fluorescence temperature-jump apparatus. The absorption wavelength is λ_1. The light path starts at the left side and passes through the sample cell, dichroic mirror and bandpass filter F_{λ_1} onto the absorption detector. The fluorescence excitation wavelength is λ_2. The light path starts at the upper right corner and is turned onto the sample cell by the dichroic mirror. 10% of energy passes onto the reference detector. The emission wavelengths are λ_3 and λ_4. Both emission detectors with bandpass and/or cut-off filters F_{λ_3} and F_{λ_4} are in parallel. Detector signals are balanced by the appropriate reference signals.

fluorescence intensity by independent optical channels. Therefore, it was possible to measure the changes of absorbance of the tRNA^{Phe} at wavelength $\lambda_1 = 280$ nm and to excite the fluorescence of the Y-base and of formycin, simultaneously at λ_2 (304 $< \lambda_2 <$ 313 nm). The experimental setup is shown in fig. 2. The light sources are 200 watt mercury lamps. The grating monochromators (Schoeffel Instruments, G 250) have an aperture ratio of 1 : 3.5 and a dispersion of 3.3 nm/mm. The dichroic mirror that superimposes the fluorescence excitation light to part of the absorption light path exhibits a reflectivity of 90% at 304 and 313 nm and also a transmittance of 90% at 280 nm (Schott u. Gen. Mainz, Germany). Filter F_{λ_1} in front of the absorption detector is a high-efficiency reflectance filter Schott UV-R 280. The overall attenuation of the excitation light at the absorption detector cathode is $<10^{-3}$. The crosstalk factors at the reference detectors are $<2\%$. Filters F_{λ_3}, F_{λ_4} in the emission light path are Schott KV 399 for emission wavelength $\lambda_3 \geqslant 399$ nm with the Y-base and Schott WG 320 + UG 11 for $\lambda_4 \approx 350$ nm with formycin. The detectors are photomultipliers with dynode switching circuits [20,21], i.e., EMI 9781 B for absorption and

references and EMI 9558 QA for emission. Changes in the fluorescence of the Y-base and formycin as a result of absorbance changes at 280 nm were found to be negligible.

We also developed a new temperature-jump cell that works at temperatures up to 90°C (fig. 3). The electrodes are constructed of platinum. A channel bored in the upper electrode houses a thermometer probe. The centerpiece is a cube constructed of polished fused silica plates which are homogeneously fused with thin black intermediate layers (Hellma, Müllheim, Germany). Two hollow half-spheres at the upper and lower sides match the electrodes. The sample cavity is 7 X 7 mm X 11 mm height, the total volume being less than 2 ml. Two lenses outside the cube together with lenses in the cell holder (fig. 2) form the emission optics. Their aperture ratio is 1 : 0.75, each providing a very high emission sensitivity. Stray light and intrinsic fluorescence are very low. Measurements of fluorescence polarization can also be performed.

The numerical analysis was carried out using an analog simulation technique. Slides of the oscilloscope traces of the temperature jump experiments were taken
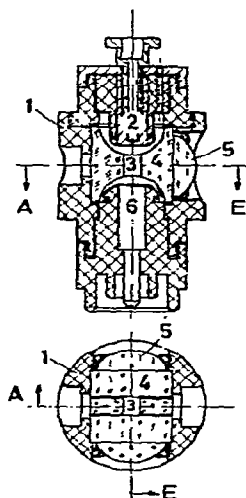
Fig. 3. Sample cell. Upper: vertical cross section, left half absorption/excitation light path, right half emission light path. Lower: horizontal cross section. (1) Cell body, (2) grounded electrode, (3) sample cavity, (4) fused silica cuvette, (5) emission lenses, (6) high-voltage electrode.

and afterwards projected on an oscilloscope screen; on the same screen the simulated time course calculated by an analog computer was displayed. The following expression for the time dependence of the intensity $I(t)$ was fit to the experimental curves:

$$I(t) = A_I \exp(-t/\tau_I) + A_{II} \exp(-t/\tau_{II}) + Bt + C .$$

The first two contributions describe two relaxation processes with the relaxation times τ_I and τ_{II} and the relaxation amplitudes A_I and A_{II}. The term Bt takes into account a nearly linear increasing base line due to cooling effects in the temperature jump cell (cf. upper trace in fig. 6) and the parameter C fits the time-independent part of the intensity.

3. Results

3.1. Equilibrium measurements

3.1.1. Fluorescence emission spectrum of tRNA^{Phe}CCF

The fluorescence spectrum of tRNA^{Phe}CCF in medium A agrees within experimental error with the

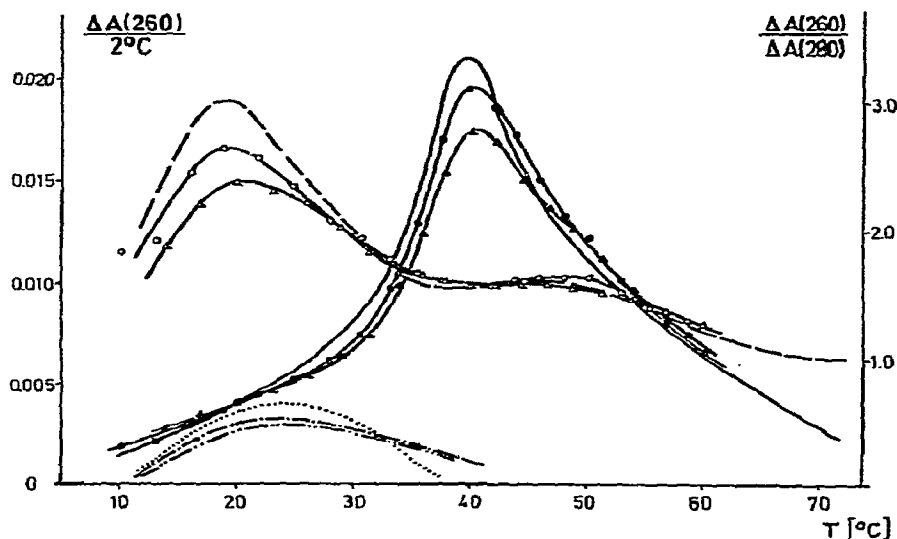Fig. 4. Differential melting curves of native and modified tRNA^{Phe} (yeast) in 0.01 M Na cacodylate, 0.02 M NaCl, 0.001 M Na EDTA, pH 6.8.
tRNA^{Phe}C$_{74}$C$_{75}$A$_{76}$: $\Delta A(260)/(\Delta 2°C)$, ——; $\Delta A(260)/\Delta A(280)$, ————; peak 1, ···; from Römer et al. [3].
tRNA^{Phe}C$_{74}$C$_{75}$: $\Delta A(260)/(2°C)$, —●—; $\Delta A(260)/\Delta A(280)$, —○—; peak 1, —·—.
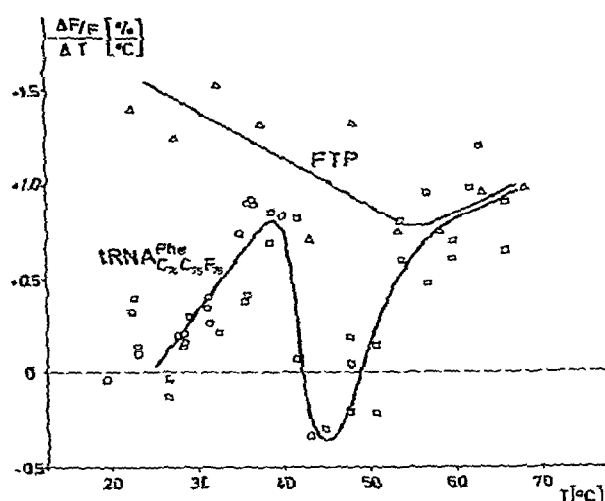tRNA^{Phe}C$_{74}$C$_{75}$F$_{76}$: $\Delta A(260)/(2°C)$, —▲—; $\Delta A(260)/\Delta A(280)$, —△—; peak 1, —··—.

Fig. 5. Temperature dependence of the relative changes of the fluorescence intensity, $(1/F)(\Delta F/\Delta T)$, of FTP and · tRNA^{Phe}C$_{74}$C$_{75}$F$_{76}$ produced by temperature differences, $\Delta T = T_2 - T_1$, in equilibrium and temperature-jump experiments. Solution conditions: 0.01 M Na cacodylate, 0.02 M NaCl, 0.001 M Na EDTA, pH 6.8. Settings of the Zeiss fluorimeter: excitation, 305 nm; emission, 335 nm; slidwidths, 2 mm. T, average temperature $(T_1 + T_2)/2$. Equilibrium measurements: FTP, $\triangle$; tRNA^{Phe}C$_{74}$C$_{75}$F$_{76}$, $\square$; T-jump measurements with tRNA^{Phe}C$_{74}$C$_{75}$F$_{76}$, $\circ$.

results of Ward et al. [11] obtained on a mixture of tRNA's from rabbit liver.

3.1.2. Melting curves

Fig. 4 shows the effect of the removal of the terminal A and its substitution by F on the melting behaviour of tRNA^{Phe} (yeast). A slight decrease of the total hypochromicity and a slight shift of some part of the main melting peak $(T_m \approx 40°C)$ is caused by the removal and reinforced by the substitution of the terminal adenosine by formycin. Peak 1 $(T_m \approx 24 \pm 1°C)$ remains virtually unchanged. The temperature dependence of the fluorescence intensity of tRNA^{Phe}CCF is quite different from the results of Ward et al. [11] with mixed tRNA from rabbit liver, but agrees with the data of Maelicke et al. [12]. First, neither in the absence nor in the presence of Mg^{++} is the fluorescence intensity higher at 80°C than at 20°C. Furthermore, a detailed investigation in the absence of Mg^{++} showed,
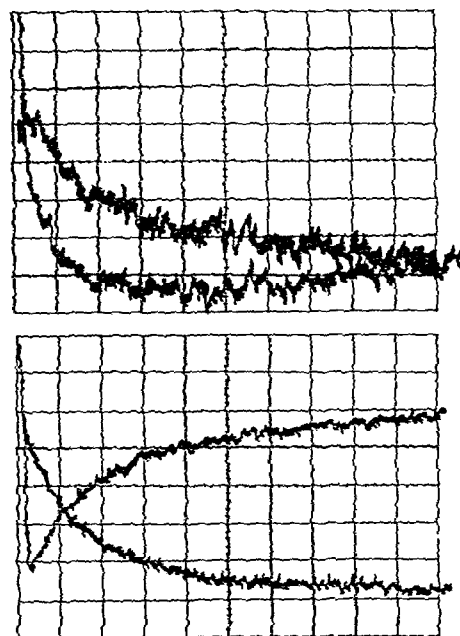

Fig. 6. Oscilloscope traces of a single temperature-jump with tRNA^{Phe}CCF monitored in the fluorescence intensity of the Y-base and of the formycin and recorded with two different time expansions. Buffer conditions: 0.01 M Na cacodylate, 0.02 M NaCl, 0.001 M Na EDTA, pH 6.8. Initial temperature 34°C; final temperature 37°C. 10 mV/division; the total signal refers to 3 V; 260 mV of the unresolvable fast intensity decrease of the Y-base are compensated.

(a) Time expansion 10 msec/division; 0.2 msec noise filter; formycin intensity upper trace, Y-base intensity lower trace.

(b) Time expansion 100 msec/division, 2.5 msec noise filter; formycin intensity with the lower final level, Y-base intensity with the upper final level.

that in the temperature interval between 20 and 70°C the fluorescence intensity decreases with increasing temperature (fig. 5), with the exception of the interval between 40°C and 50°C where a small increase was observed. Because of the considerable scattering of the experimental values in fig. 5 the interpolated lines give only the salient features such as the minimum and the maximum in the changes of fluorescence intensity of tRNA^{Phe}CCF. The appearance of the maximum and the minimum is also strongly supported by the temperature-jump amplitudes. The decrease of the fluorescence intensity of FTP with increasing temperature is

qualitatively similar as with the nucleoside formycin. Quantitatively this quenching is only about half as efficient in FTP as in the nucleoside. However, it is still much stronger than in tRNA^{Phe}CCF.

3.2. Temperature-jump studies

Temperature-jump experiments were carried out in the standard media given in section 2.6. Under both conditions, there is a particular temperature range (see below) where besides a fast and unresolved (faster than 5 μsec) effect two well resolved relaxation effects were observed: a faster one (relaxation time τ_I and amplitude A_I) in the range of 10 msec, and a slower one (τ_{II}, A_{II}) in the range of 100 msec. An oscillogram is shown in fig. 6. Both relaxation effects can be observed by monitoring either the formycin cr Y-base fluorescence, or the UV absorbance. The relaxation times evaluated independently from the three observation methods are identical within the limits of error.

3.2.1. Amplitudes

Both relaxation effects were followed over a wide

Table 2
Relaxation times of tRNA^{Phe}CCF in 0.01 M sodium-cacodylate, 5×10^{-4} M EDTA, pH 6.8

T (°C)	τ_I (msec)	τ_{II} (msec)
a)		
25.7	65 (± 8)	1.550 (± 150)
29.3	30 (± 3)	1.150 (± 150)
29.7	20 (± 4)	800 (± 100)
32.5	8 (± 1)	
32.9	7 (± 1)	440 (± 50)
37.0		100 (± 20)
b) 0.02 M NaCl added		
32.7	23.5 (± 3)	475 (± 40)
36.2	10.0 (± 1)	205 (± 10)
37.7	5.9 (± 0.5)	165 (± 8)
38.5	5.5 (± 0.8)	150 (± 10)
41.2		85 (± 5)
41.8	3.0 (± 0.3)	85 (± 5)
44.5		24 (± 2)
45.3	1.6 (± 0.2)	25 (± 3)
45.6	2.2 (± 0.4)	17 (± 2)

temperature range (table 2). The dependences of the amplitudes upon temperature are shown in fig. 7. Above 38°C under conditions of fig. 7a and above 45°C under conditions of fig. 7b the total amplitude corresponds to the unresolved effect. Whereas the fluorescence intensity of the formycin label decreases during both resolved relaxation effects, the fast resolved decrease of the Y-base fluorescence is followed by a slow increase (figs. 6 and 7). The temperatures where the maxima of the amplitudes were observed are very similar for all methods of observation. They coincide with peak 2 determined earlier in the UV-absorbance melting curve under the same conditions [3]. The total amplitudes correspond to the values of the differential melting curve determined from the equilibrium measurements (fig. 5). In addition to the two relaxation processes we cannot exclude a small contribution from an effect in the 100 μsec range (τ_{III}), which may be responsible for the initial curvature of the oscilloscope trace of the formycin fluorescence (fig. 6). This effect is too small to be evaluated quantitatively.

The signs of the relaxation amplitudes A_I and A_{II} and their ratio A_I/A_{II} are independent of the wavelength of observation demonstrating that the intensity changes are not due to a spectral shift of the emission band.

3.2.2. Relaxation times

The relaxation times of both resolvable effects are listed in table 2 for different temperatures and at two ionic strengths. Each value represents an average value obtained from measurements monitoring the formycin and Y-base fluorescence and the UV absorbance. As mentioned above, the use of the different modes of observation resulted in identical relaxation times within the limits of error. It will be described in detail in the discussion, how it is not possible, without restrictive assumptions, to derive a set of rate constants from two or more simultaneously observed relaxation times. The relaxation times have been found to be independent of tRNA concentration. T-jumps obtained of the Y-base fluorescence of tRNA^{Phe}CCA and tRNA^{Phe}CCF under otherwise identical conditions yielded very similar amplitudes and relaxation times. This result shows that the fluorescence of the Y-base is not significantly affected by energy transfer from the formycin fluorescence.
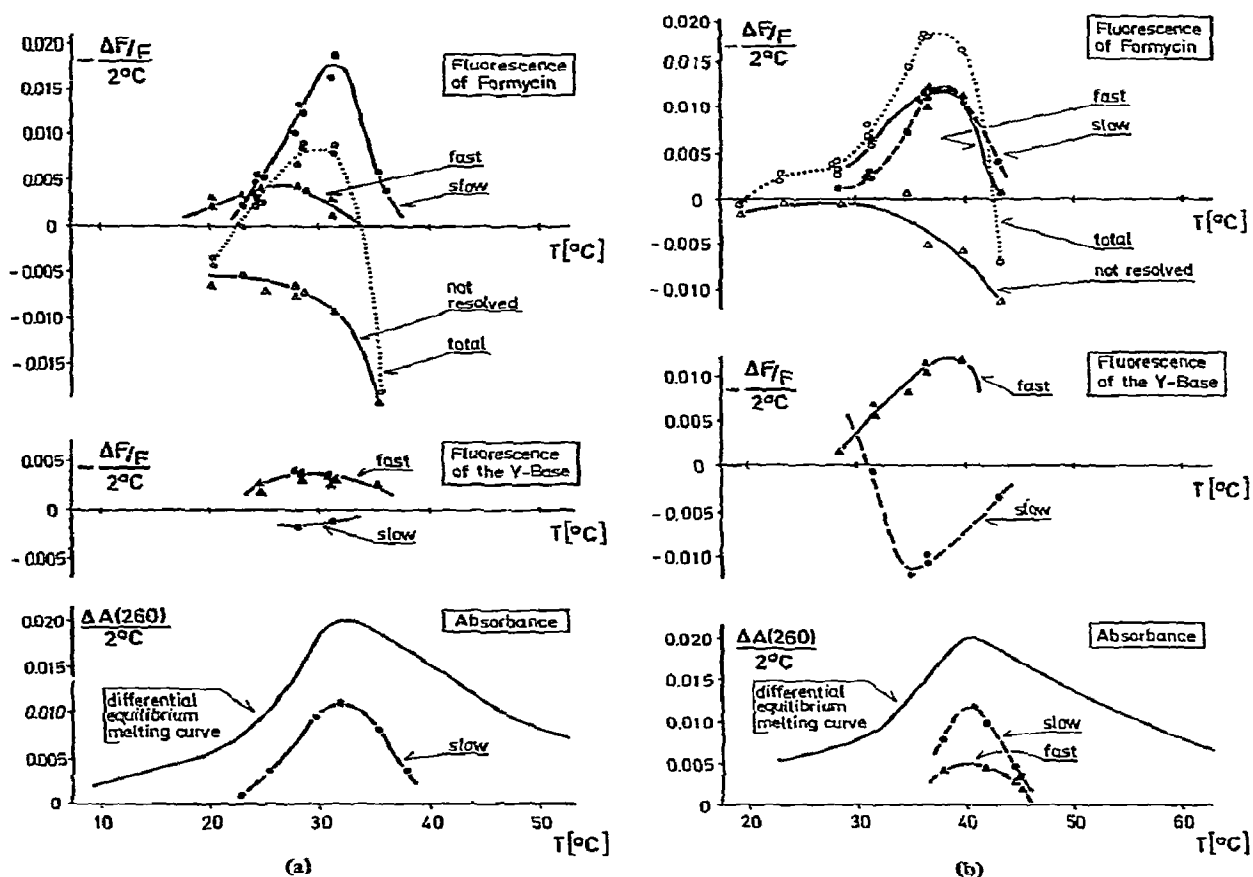
Fig. 7. Dependence of the temperature-jump amplitudes upon temperature. (a) tRNA^{Phe}CCF in 0.01 M Na cacodylate, 10^{-4}M Na EDTA, pH 6.8; (b) 0.02 M NaCl added. The absorbance measurements were carried out with tRNA^{Phe}CCA.

4. Discussion

4.1. Methodological aspects

In earlier fast kinetic studies on fragments and intact tRNA's from various species we have discussed the possibility of distinguishing between fast, uncooperative stacking equilibria and cooperative helix—coil transitions. The measurement of the relaxation amplitudes as a function of temperature allows a direct determination of the melting profiles of the individual processes. Thus, the amplitude of the single strand stacking equilibrium could be determined directly and its contribution could be separated from the double helix—

coil transitions [22—24]. Later on, the same method has been used extensively in the study of synthetic oligonucleotides [25,26].

In this paper we have applied the same principle to the fluorescence measurements observed with a modified fluorescence T-jump apparatus. For example, the dependence of the fluorescence intensity of the Y-base on temperature is determined mainly by a fast, unspecific fluorescence quenching. On the other hand, the T-jump amplitude data in fig. 7 clearly exhibit two resolvable processes besides the fast and unspecific effect. In addition, it is remarkable that the relaxation signal obtained by monitoring the Y-base exhibits two resolvable phases with opposite signs. At infinite time

the two amplitudes (A_I, A_{II}) compensate each other almost completely. This explains why equilibrium measurements on the Y-base fluorescence are relatively insensitive to these cooperative changes. The Y-base fluorescence is particularly well suited to demonstrate the advantage of the T-jump technique in determining thermodynamic data of tRNA melting as compared with conventional melting techniques. T-jump studies combine the higher resolution of the differential technique and the advantage of a higher signal to noise ratio with a separation of the individual processes on the time axis.

4.2. Does the formycin label influence the structure of the tRNA-molecule?

As judged by the UV-melting profiles of tRNA^{Phe}CCA, tRNA^{Phe}CC and tRNA^{Phe}CCF, modification of the 3'-end induces no major changes in tRNA conformation. The only changes observed in the melting profiles of the modified molecules are a slight stabilization of the main melting peak and a small loss of the total hypochromicity (fig. 4). Most important, however, the unfolding of tertiary structure in peak 1 is virtually unchanged. Furthermore, the relaxation processes monitored by the Y-base fluorescence are not changed by substituting the terminal adenosine by formycin. Also, the finding that tRNA^{Phe}CCF can be fully aminoacylated shows that the conformation of the tRNA is virtually unchanged by the fluorescence label [11, 12].

4.3. Relaxation amplitudes monitored by the fluorescence labels

Fluorescence labels in tRNA may be used to monitor conformational changes in the cloverleaf branch where the label is incorporated, or the unfolding of the tertiary structure. It is known that transition 1 in the UV-absorbance melting curve of tRNA^{Phe} represents unfolding of the tertiary structure [4,5]. In the temperature range of this transition no resolved relaxation effect was observed in the fluorescence intensity of the Y-base as well as that of the formycin. This shows that the CCA end and the anticodon loop are not involved in the main part of the tertiary structure (c.f. section 4.5). A similar result with respect to the CCA end was obtained by comparison of the fluorescence of

formycin incorporated in oligonucleotides and in native and denatured tRNA [12,27]. Our conclusions are compatible with results obtained by a variety of methods such as enzymatic digestions, chemical modifications, oligonucleotide binding, thermodynamic and spectroscopic studies and X-ray analysis.

It has been shown that of the hU and rT stem each gives raise to a well resolved relaxation in the upper part of the melting curve [2]. Since in this temperature range no resolved fluorescence relaxation has been observed it can be concluded that the disruption of these stems does not affect the fluorescence intensity of either the Y-base or the formycin.

The absence of fluorescence changes in the previously assigned parts of the melting curves as well as the appearance of fluorescence changes in the temperature range of effects 2 and 3 (fig. 8) leads to the assignment of effects 2 and 3 to the dissociation of the acceptor- and anticodon stems. Since in the fluorescence and UV absorbance measurements the relaxation times and the temperature range of the amplitudes agree quantitatively it is evident that identical processes have been observed. The amplitudes of the two resolved relaxation effects monitored by the fluorescence intensity of the Y-base have opposite signs and almost cancel each other throughout the temperature interval where they can be observed (fig. 7). It follows that the superimposition of the two relaxation effects causes no net decrease of the fluorescence intensity over the temperature range of the corresponding cooperative transitions. This result cannot be due to energy transfer between formycin and the Y-base because it is found in tRNA^{Phe}CCA as well as in tRNA^{Phe}CCF. It can be understood, however, on the basis of structural changes of tRNA^{Phe}CCA. From studies on tRNA fragments it is known that the dissociation of the anticodon stem results in a decrease of the fluorescence intensity of the Y-base [5]. Therefore, the absence of a net decrease during the melting of the total tRNA molecule shows that the melting of the anticodon stem is not the only process giving rise to the fluorescence changes of the Y-base. This assumption is difficult to visualize without postulating some kind of conformational element not included in the ordinary cloverleaf model. Hence, we speculate that even after the unfolding of tertiary structure in peak 1 there is some residual tertiary structure present. Then the dissociation of this structure would increase the fluorescence of the

Y-base by about the same amount as the dissociation
of the anticodon stem lowers the fluorescence. The
persistence of some kind of conformational element
in addition to the cloverleaf branches even after the
unfolding of tertiary structure in peak 1 has also been
inferred from studies on the influence of organic sol-
vents on the melting behaviour of tRNA^{Phe} [28].

In discussing the relaxation amplitudes as observed
by the fluorescence of the terminal formycin two
general fluorescence properties of the formycin label
have to be considered [11,12]. First, the normal
quenching of fluorescence produced by raising the
temperature and second, a conformational quenching
as a consequence of the incorporation of formycin
into oligo- and polynucleotides. The resolved relaxation
effects reported in this paper are connected with a de-
crease of the fluorescence intensity (fig. 7), and they
may be interpreted as arising from an increase in the
conformational quenching. From this argument one
would expect that a release of conformational quench-
ing would then lead to an increase of fluorescence in-
tensity. This is indeed observed in the appearance of a
positive unresolved relaxation shifted to higher tem-
peratures as compared to the resolved relaxation ef-
fects. Finally at temperatures higher than 50°C the
fast unresolved relaxation becomes negative and also
quantitatively very similar to the normal temperature
quenching as observed in FTP.

4.4. Coupling

Since the CCA- and anticodon branches melt out
in the same temperature range, information about
their mutual interaction may be obtained from the
corresponding relaxation data. If there is no interac-
tion between the two branches the two melting
processes are simply superimposed both in the equili-
brium and temperature-jump measurements. This
means that each relaxation is clearly correlated to
just one of the processes and is monitored by the
fluorescence label sensitive to this process only.
Quite a different relaxation behaviour has to be ex-
pected if the anticodon and acceptor branches are
coupled in the sense that the presence of one double
helical stem stabilizes the other one. For example,
some interactions between the two cloverleaf branches
can actually be predicted by ring-closure arguments
[29,30]. Melting of the acceptor stem opens the central

ring of the molecule and therefore destabilizes the anti-
codon branch. An estimate of this effect, however, is
very difficult, particularly since the influence of the
residual tertiary structure postulated above can hardly
be assessed. Experimentally, coupling should clearly
show up in the relaxation behaviour. Each of the relaxa-
tion processes observed in a coupled system is no longer
directly correlated to the individual reaction steps but
to linear combinations of the extents of reaction of
these steps [19]. As a consequence, all relaxation
processes will show up in the signal of a label whose
spectroscopic properties are influenced by one reaction
step only.

In our particular case a coupled opening of the ac-
ceptor- and anticodon branches accounts well for the
experimental finding that the two relaxation times of
our system are observed on both of the fluorescence
labels. An uncoupled melting of the two cloverleaf
branches, on the other hand, would be compatible
with the measured relaxation curves only if additional
assumptions were made, e.g., that each of the two
labels on distant parts of the molecule would have to
be directly sensitive to conformational changes in the
environment of the other one. For the Y-base we had
to postulate (vide supra) that it does not only monitor
the anticodon branch but also some residual tertiary
structure probably melting concomitantly with the
acceptor stem. However this does not necessarily
imply a similar sensitivity of the formycin label to
the disruption of the anticodon stem. On the contrary,
such an additional complication is not warranted,
since the relaxation monitored by the fluorescence
of the terminal formycin is readily explained by the
expected coupling of the acceptor and anticodon
stems.

For a more quantitative discussion of the coupled
mechanism we have to introduce several approximation.
It has been mentioned that a third relaxation time was
observed in the corresponding temperature range. This
effect, however, has a very small amplitude and it was
not possible to decide whether or not it is due to dif-
ferent intermediate states during the denaturation of
the acceptor and anticodon branches or is simply a
relic of the other denaturation steps. Therefore, the
third relaxation effect is not included in the analysis
below.

Although the fluorescence amplitudes have been
useful in the qualitative interpretation of the different

melting steps, they hardly allow one to calculate concentration changes without additional assumptions, because the quantum-yields involved and their strong dependences upon temperature are not known. For a quantitative treatment the relaxation amplitudes measured in UV absorbance together with the relaxation times and their temperature dependences are used.

Since just two relaxation times are observed, only one intermediate needs to be considered. The knowledge of two relaxation times and their amplitudes allows the determination of the rate constants of a mechanism no more complicated than the following:

$$X_1 \underset{k_{21}}{\overset{k_{12}}{\rightleftharpoons}} X_2 \underset{k_{32}}{\overset{k_{23}}{\rightleftharpoons}} X_3 .$$
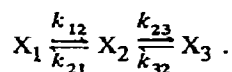
This scheme implies that two of the three structural elements, i.e., residual tertiary structure, acceptor and anticodon branch, have to be included in one step. Dissociation of residual tertiary structure and the anticodon branch in one step can be ruled out because their almost equal but opposite influence on the Y-base would cancel each other throughout the relaxation process, which would be incompatible with the relaxation effects observed.

Since the physico-chemical parameters of the residual tertiary structure are not known, we tried to fit the experimental data to the reaction scheme without taking into account this structure.

Thus, two alternative intermediates remain: either the acceptor branch opens up first with the anticodon branch being still closed or vice versa. The mathematical procedure used in this analysis is described in the appendix. The values of the hypochromicities and reaction enthalpies needed for the calculation are taken from the literature [2]. From these calculations it turns out that the assumed intermediates do not lead to a self consistent fit of the temperature dependence of the data. This result supports the conclusion derived from the fluorescence amplitudes, that some additional non-cloverleaf conformation is involved in the melting processes of the acceptor and anticodon branches.

4.5. Synopsis and comparison with previous results

Fig. 8 which shows the five melting transitions in tRNA^Phe (yeast) summarizes the results of this and previous papers. Peak 1 has been assigned to tertiary structure melting. The results of this paper lead to the
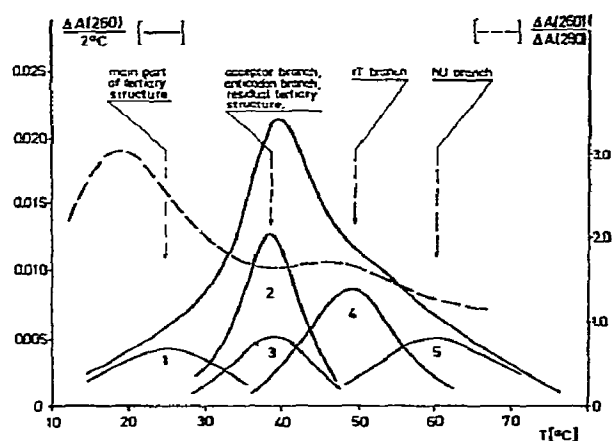

Fig. 8. Summary of the five conformational transitions of tRNA^Phe (yeast) in 0.01 M Na cacodylate, 0.001 M Na EDTA, 0.02 M NaCl, pH 6.8.

conclusion that some form of tertiary structure is also involved in peaks 2 and 3. The most obvious properties, however, which one would expect for tertiary structure are observed in peak 1:

(a) it contains steric constraints for the intercalation of ethidiumbromide into the cloverleaf stems, i.e., its presence abolishes about half of the strong binding sites for the dye [4];

(b) the dependence of its T_m upon ionic strength is stronger than in all known double-helices [2];

(c) it provides five strong binding sites for Mg^{2+} [17]; and

(d) it plays the role of a structural lock: it provides thermodynamic stability, and its recombination constitutes the rate limiting step for the formation of the native conformation [2–5].

The participation of some form of the tertiary structure in effects 2 and 3 has been inferred only indirectly. Therefore we call it residual tertiary structure as opposed to the main part of tertiary structure involved in peak 1.

The scheme of five melting transitions is in fact complete with respect to reaction enthalpy because it accounts quantitatively for the overall heat of melting observed calorimetrically [31,32], although the calorimetric data appear to disagree somewhat under conditions of low ionic strength [31–34]. Solution conditions, in particular the concentration of mono- and divalent salts, strongly influence the relative posi-

tions of the melting transitions on the temperature scale. For example in the presence of Mg^{++} very steep melting profiles are observed, where the five transitions are no longer resolved as in fig. 8, but are superimposed to a greater extent and are coupled by the influence of peak 1.

In contrast to the UV-absorption and fluorescence detection, which was used in this work, NMR experiments have indicated that the dissociation of all cloverleaf branches of tRNA^{Phe} (yeast) occurs over a very narrow temperature range [35]. If we extrapolate our temperature jump results to the conditions of the NMR experiments according to the method outlined in ref. [36], the superimposition of the different melting effects as observed by NMR is in fact expected. The thermodynamic and kinetic properties of tRNA^{Phe}(yeast) are thus particularly unfavorable for the resolution of the melting transitions by the NMR method.

Other tRNA molecules which have been investigated in a comparably detailed manner [tRNA^{Ala}(yeast) [18], tRNA^{Tyr}(E. coli) [37,38], tRNA^{fMet}(E. coli) [36], and tRNA^{Asp}(yeast) [39]] have also shown an early melting effect with similar thermodynamic properties of those of peak 1 of tRNA^{Phe} (yeast).

One may generalize that unfolding of the main part of tertiary structure is the first denaturation step in all tRNA's. It may not be possible in all cases, however, to find conditions where the tertiary structure is unfolded and all of the branches of the clover leaf are still double helical as in tRNA^{Phe}(yeast). In tRNA^{fMet}(E. coli) [38] and tRNA^{Asp}(yeast) [39] the hU stem is too unstable to exist in the double helical state after tertiary structure has unfolded. Also, the order in which the different cloverleaf branches subsequently melt out is not a common feature of all tRNA molecules, but reflects rather the thermodynamic properties of the nucleotide sequences, numbers of possible base pairs and loop sizes of the particular tRNA species.
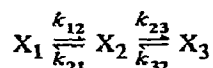
Many theoretical attempts have been made to predict the thermodynamics of a tRNA from its nucleotide sequence. Most of the theoretical results for tRNA^{Phe} (yeast) [40] agree with our experimental results.

Acknowledgement

Appendix

In order to evaluate the rate constants of the mechanism

$$X_1 \underset{k_{21}}{\overset{k_{12}}{\rightleftharpoons}} X_2 \underset{k_{32}}{\overset{k_{23}}{\rightleftharpoons}} X_3$$

from two relaxation times (τ_I, τ_{II}) and two relaxation amplitudes (A_I, A_{II}) four equations are needed. The formulas for the sum and the product of the reciprocal relaxation times are taken from [19]:

$$\frac{1}{\tau_I} + \frac{1}{\tau_{II}} = k_{12} + k_{21} + k_{23} + k_{32},$$ (A.1)

$$\frac{1}{\tau_I} \times \frac{1}{\tau_{II}} = k_{12}k_{23} + k_{32}(k_{12} + k_{21}).$$ (A.2)

An overall degree of transition is defined in the following way:

$$\theta(T) = \frac{\displaystyle\int_{T_0}^{T} (A_I + A_{II}) \, dT'}{\displaystyle\int_{T_0}^{T_1} (A_I + A_{II}) \, dT'} = \frac{(\epsilon_2 - \epsilon_1) C_2 + (\epsilon_3 - \epsilon_1) C_3}{(\epsilon_3 - \epsilon_1)(C_1 + C_2 + C_3)}.$$

T_1 and T_0 are temperatures above and below the transition range and ϵ_1, ϵ_2, ϵ_3 and C_1, C_2, C_3 are the extinction coefficients and the concentrations of molecules in the states X_1, X_2, and X_3, respectively. With

$$C_2/C_1 = k_{12}/k_{21} \quad \text{and} \quad C_3/C_2 = k_{23}/k_{32}$$

it follows, that

$$\frac{\int_{T_0}^{T} (A_I + A_{II})\, dT'}{\int_{T_0}^{T_1} (A_I + A_{II})\, dT'} = \frac{[(\epsilon_1 - \epsilon_2)/(\epsilon_1 - \epsilon_3)]\,(k_{12}/k_{21}) + (k_{12}/k_{21})\,(k_{23}/k_{32})}{1 + (k_{12}/k_{21}) + (k_{12}/k_{21})(k_{23}/k_{32})} \cdot \tag{A.3}$$
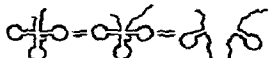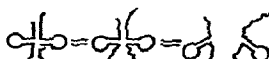
The fourth equation is taken from the ratio of the amplitudes as derived in [2]:

$$\frac{A_I}{A_{II}} = -\frac{(\epsilon_3 - \epsilon_2)k_{23} + (\epsilon_1 - \epsilon_2)(k_{12} + k_{21} - 1/\tau_{II})}{(\epsilon_3 - \epsilon_2)(k_{23} + k_{32} - 1/\tau_I) + (\epsilon_1 - \epsilon_2)k_{21}}$$

$$\times \frac{k_{21}[(1 + k_{12}/k_{21}) + \Delta H_{12}/\Delta H_{23}] + (k_{23} + k_{32} - 1/\tau_I)[1 + (1 + k_{32}/k_{23})\Delta H_{12}/\Delta H_{23}]}{(k_{12} + k_{21} - 1/\tau_{II})[(1 + k_{12}/k_{21}) + \Delta H_{12}/\Delta H_{23}] + k_{23}[1 + (1 + k_{32}/k_{23})\Delta H_{12}/\Delta H_{23}]} \cdot \tag{A.4}$$

Besides the four temperature-dependent rate constants the equations contain two temperature-independent parameters, the ratio of the extinction differences $(\epsilon_1 - \epsilon_2)/(\epsilon_2 - \epsilon_3)$ and the ratio of the reaction enthalpies $\Delta H_{12}/\Delta H_{23}$. For a particular reaction model involving definite double helical regions (see table A.1) the temperature-independent

Table A.1
Inconsistency of simplified models and experimental results. Ratios of reaction enthalpies for tRNA^{Phe} obtained from relaxation experiments $(\Delta H_{12}/\Delta H_{23})$ are compared with theoretical data $(\Delta H_{12}/\Delta H_{23})_{th}$

Model	$[(\epsilon_1 - \epsilon_2)/(\epsilon_2 - \epsilon_3)]_{th}$	$(\Delta H_{12}/\Delta H_{23})_{th}$	$\Delta H_{12}/\Delta H_{23}$
	1.6	1.25	−0.2
	0.65	0.8	0.1

parameters can be estimated by summing up the hypochromicities [2,41] and reaction enthalpies [2] of the corresponding base pairs. These theoretical values $(\epsilon_1 - \epsilon_2)/(\epsilon_2 - \epsilon_3)_{th}$, $(\Delta H_{12}/\Delta H_{23})_{th}$ are used as a starting point for the calculation of the four rate constants from eqs. (A.1)–(A.4). From the temperature dependence of the equilibrium constants $K_1 = k_{12}/k_{21}$ and $K_2 = k_{23}/k_{32}$ obtained in this way new reaction enthalpies ΔH_{12} and ΔH_{23} were calculated. The consistency of the experimental results and the theoretical model data for the reaction enthalpies and absorbance changes was tested by comparing $(\Delta H_{12}/\Delta H_{23})_{th}$ with $\Delta H_{12}/\Delta H_{23}$. Evidently, the calculations rule out the two models discussed in table A.1. Intermediates involving partially unfolded clover leaf branches were found to be consistent with the experimental data. However, they are not included in the table, since they do not account for the essential features of the residual tertiary structure.

References

[1] F. Cramer, in: Progress in Nucleic Acid Research and Molecular Biology, eds. J.N. Davidson and W.E. Cohn (Academic Press, London and New York, 1971) Vol. 11, p. 391.

[2] D. Riesner and R. Römer, in: Physico-chemical Properties of Nucleic Acids, ed. J. Duchesne (Academic Press, London and New York, 1973) Vol. 2, p. 237.

[3] R. Römer, D. Riesner and G. Maass, FEBS Letters 10 (1970) 352.

[4] C. Urbanke, R. Römer and G. Maass, Eur. J. Biochem. 23 (1973) 511.

[5] D. Riesner, G. Maass, R. Thiebe, P. Philippsen and H.G. Zachau, Eur. J. Biochem. 36 (1973) 76.

[6] R.G. Shulman, C.W. Hilbers, Y.P. Wong, K.L. Wong, D.R. Lightfoot, B.R. Reid and D.R. Kearns, Proc. Nat. Acad. Sci. USA 70 (1973) 2042.

[7] U.L. Raj Bhandary, S.H. Chang, A. Stuart, R.D. Faulkner, R.M. Hoskinson and H.G. Khorana, Proc. Nat. Acad. Sci. USA 57 (1967) 751.

[8] J. Eisinger, B. Feuer and T. Yamane, Proc. Nat. Acad. Sci. USA 65 (1970) 638.

[9] K. Beardsley, T. Tao and C.R. Cantor, Biochemistry 9 (1970) 3524.

[10] R. Thiebe and H.G. Zachau, Biochem. Biophys. Acta 217 (1970) 294.

[11] D.C. Ward, E. Reich and C. Stryer, J. Biolog. Chem. 244 (1969) 1228.

[12] A. Maelicke, M. Sprinzl, F. von der Haar, T.A. Khwaja and F. Cramer, Eur. J. Biochem. 43 (1974) 617.

[13] H. Sternbach, F. v.d. Haar, E. Schlimme, E. Gaertner and F. Cramer, Eur. J. Biochem. 22 (1971) 166.

[14] R.J. Mans and G.D. Novelli, Arch. Biochem. Biophys. 94 (1961) 48.

[15] H. Fraenkel-Conrat and A. Steinschneider, Methods Enzym. XII (B) (1968) 243.

[16] M.P. Deutscher, J. Biol. Chem. 247 (1972) 469.

[17] R. Römer and R. Hach, Eur. J. Biochem. 55 (1975) 271.

[18] R. Römer, D. Riesner, S.M. Coutts and G. Maass, Eur. J. Biochem. 15 (1970) 77.

[19] M. Eigen and L. De Maeyer, in: Techniques of Organic Chemistry, ed. A. Weissberger (Wiley, New York, 1963) Vol. VIII/2, ch. 18.

[20] R. Rigler, C.R. Rabl and T.M. Jovin, Rev. Sci. Instr. 45 (1974) 580.

[21] C.R. Rabl, in: Dechema Monographien "Technische Biochemie", ed. H.J. Rehm (Verlag Chemie, Weinheim, 1973) Vol. 71, p. 187.

[22] D. Pörschke, Thesis, University of Braunschweig (1969).

[23] R. Römer, D. Riesner, G. Maass, W. Wintermeyer, R. Thiebe and H.G. Zachau, FEBS Letters 5 (1969) 15.

[24] D. Riesner, R. Römer and G. Maass, Eur. J. Biochem. 15 (1970) 85.

[25] J. Gralla and D.M. Crothers, J. Mol. Biol. 78 (1973) 301.

[26] J. Ravetch, J. Gralla and D.M. Crothers, Nucleic Acids Research 1 (1974) 109.

[27] R.D. Irwin and J.G. Chirikjian, Federation Proceedings, Vol. 32 (1973) 617, Abs. 2268.

[28] K. Weber, Diplomarbeit, Universität Braunschweig (1973).

[29] I.E. Scheffler, E.L. Elson and R.L. Baldwin, J. Mol. Biology 48 (1970) 145.

[30] C. DeLisi and D.M. Crothers, Biopolymers 10 (1971) 1809.

[31] N.G. Bakradze, J.R. Monaselidze, G.M. Mrevlishvili, A.D. Bibikova and L.L. Kisselev, in: Conformation Changes of Biopolymers in Solutions (Nauka, Moscow, 1973).

[32] D. Bode, U. Schernau and Th. Ackermann, Biophys. Chem. 1 (1974) 214.

[33] J. Levy, G. Rialdi and R. Biltonen, Biochemistry 11 (1972) 4138.

[34] J.F. Brandts, W.M. Jackson and T. Yao-Chung Ting, Biochemistry 13 (1974) 3595.

[35] C.W. Hilbers, R.G. Shulman and S.H. Kim, Biochem. Biophys. Res. Commun. 55 (1973) 953.

[36] D.M. Crothers, P.E. Cole, C.W. Hilbers and R.G. Shulman, Biochemistry 87 (1974) 63.

[37] P.E. Cole, S.K. Yang and D.M. Crothers, Biochemistry 11 (1972) 4358.

[38] E. Schultz, Diplomarbeit, Universität Braunschweig (1973).

[39] S.M. Coutts, M. Gangloff and G. Dirheimer, Biochemistry 13 (1974) 3938.

[40] C. DeLisi, Biopolymers 12 (1973) 1713.

[41] J.R. Fresco, L.C. Klotz and E.G. Richards, Cold Spring Harbor Symp. Quant. Biol. 28 (1963) 83; J.R. Fresco, personal communication.